RESEARCH ARTICLE



Design, microwave-assisted synthesis, biological evaluation and molecular modeling studies of 4-phenylthiazoles as potent fatty acid amide hydrolase inhibitors

Stephanie R. Wilt [©] | Mark Rodriguez | Thanh N. H. Le | Emily V. Baltodano | Adrian Salas | Stevan Pecic D

Department of Chemistry and Biochemistry, California State University-Fullerton, Fullerton, CA, USA

Correspondence

Stevan Pecic, Department of Chemistry and Biochemistry, California State University-Fullerton, Fullerton, CA 92834, USA. Email: specic@fullerton.edu

Funding information

Project RAISE, U.S. Department of Education HSI-STEM, Grant/Award Number: P031C160152; National Science Foundation MRI. Grant/Award Number: CHE1726903; College of Natural Sciences and Mathematics at California State University, Fullerton

Abstract

Endocannabinoids, anandamide (AEA) and 2-arachidonoylglycerol (2-AG), are endogenous lipids that activate cannabinoid receptors. Activation of these receptors produces anti-inflammatory and analgesic effects. Fatty acid amide hydrolase (FAAH) is a membrane enzyme that hydrolases endocannabinoids; thus, inhibition of FAAH represents an attractive approach to develop new therapeutics for treating inflammation and pain. Previously, potent rat FAAH inhibitors containing 2-naphthyl- and 4-phenylthiazole scaffolds were identified, but up to the present time, very little structure-activity relationship studies have been performed on these moieties. We designed and synthesized several analogs containing these structural motifs and evaluated their inhibition potencies against human FAAH enzyme. In addition, we built and validated a homology model of human FAAH enzyme and performed docking experiments. We identified several inhibitors in the low nanomolar range and calculated their ADME predicted values. These FAAH inhibitors represent promising drug candidates for future preclinical in vivo studies.

KEYWORDS

docking experiments, enzyme inhibition, homology modeling, microwave-assisted synthesis, structureactivity relationship study

1 INTRODUCTION

CB1 and CB2 are cannabinoid receptors are present in the central nervous system and the peripheral nervous system, respectively (Davis, 2014; Pertwee, 2006). Cannabinoid receptors are activated by cannabinoid chemical compounds, which play an important role in the regulation of many physiological processes, including pain and inflammation (Basavarajappa, 2017). There are three known classes of cannabinoids: phytocannabinoids, synthetic cannabinoids, and endocannabinoids. Phytocannabinoids are natural products found in Cannabis sativa, such as Δ^9 -tetrahydrocannabinol (THC)—one of the active ingredients of marijuana (Thomas & ElSohly, 2016). To the second group of cannabinoids, synthetic cannabinoids, belong chemically synthesized cannabinoid receptor agonists. Most synthetic cannabinoids are intended to mimic the natural cannabinoids, for example CP-47497, without containing the typical phytocannabinoid bicyclic structure (Hruba & McMahon, 2017; Le Boisselier, Alexandre, Lelong-Boulouard, & Debruyne, 2017). Several recent studies evaluated prolonged exposures of mice to synthetic cannabinoids and their impact on recognition memory and brain metabolism overall (Mouro et al., 2019; Mouro, Ribeiro, Sebastião, & Dawson, 2018). Endocannabinoids are endogenous lipid ligands, the non-plant-based neurotransmitters that are naturally produced in the mammalian body (Okamoto, Wang, Morishita, & Ueda, 2007; Simon & Cota, 2017). Two main endocannabinoids are anandamide (AEA) and 2-arachidonoylglycerol (2-AG). By

© 2020 John Wiley & Sons A/S.

the activation of the CB1 and CB2 receptors, AEA produces a similar pain alleviation effect, such as analgesia, anti-inflammation, anxiolysis, and anti-depression effects, without giving undesirable side-effects as THC or synthetic cannabinoids, including cognitive and motor impairments (Ahn, Johnson, & Cravatt, 2009; Scherma et al., 2019). However, AEA is only synthesized on-demand, when there are inflammation and immune responses, and is rapidly metabolized by the enzyme fatty acid amide hydrolase (FAAH), which is a mammalian integral membrane enzyme (Bisogno & Maccarrone, 2013; Morena et al., 2019). FAAH enzyme metabolizes AEA by hydrolyzing it to the arachidonic acid and ethanolamine (Figure 1a); therefore, FAAH is mainly responsible for the termination of anandamide signaling in vivo (Reggio, 2010). The FAAH enzyme belongs to a large group of enzymes called amidase signature (AS), which is known to share a highly conserved sequence homology structure among diverse species (Lu & Anderson, 2017; Ueda, 2002). The X-ray crystallographic structure of the rat FAAH enzyme shows that FAAH possesses an unusual serine-serine-lysine (Ser241-Ser217-Lys142) catalytic triad (McKinney & Cravatt, 2003). The mechanism of the hydrolytic cleavage of the amide bond by the FAAH enzyme has been proposed by Ahn et al. (Ahn, Johnson, Mileni, et al., 2009). In short, once the substrate AEA enters the active site of FAAH, its amide bond will be in the close proximity of Ser241 residue. In the first step of the postulated mechanism, Lys142 acts as a base and is protonated by Ser217, followed by the proton transfer from Ser241 to Ser217. Ser241 becomes a nucleophile and attacks the carbonyl part of the amide bond of the substrate AEA. In the next step, Ser217 acts as an acid and donates a proton to the nitrogen atom of the amide substrate, giving it a partially positive charge and making it a good leaving group. An acyl-enzyme intermediate containing Ser241 and the carbonyl product is formed, with the simultaneous sharing of a proton

(a)
$$Lys142$$

$$Ser217$$

$$Ser241$$

$$Anandamide (active)$$
(b)
$$L142$$

$$Ser217$$

$$Arachidonic acid (inactive)$$

$$Ser241$$

FIGURE 1 (a) Inactivation of endocannabinoid anandamide and catalytic triad of fatty acid amide hydrolase (FAAH). (b) Mechanism of the hydrolytic cleavage of anandamide

between Lys142 and Ser217. The intermediate then reacts with a water molecule, which eventually releases the free fatty acid product—arachidonic acid. Lys142, Ser217, and Ser241 then return to their initial protonation states (Figure 1b).

1.1 Known FAAH inhibitors

There are several distinct groups of FAAH inhibitors discovered up to date, including reversible and irreversible inhibitors (Figure 2). The first investigated group of FAAH inhibitors were substrate-derived inhibitors, such as the reversible inhibitor trifluoromethyl ketone analog of oleamide 1, with reported K_i of 82 nM (Boger et al., 1999). These substrate-based FAAH inhibitors are highly hydrophobic, have low selectivity, and did not present good lead compounds for future drug development. The next explored group of FAAH inhibitors were α-ketoheterocycles. These inhibitors were more selective and more potent. One of the very potent inhibitors from this group is OL-135 2, with K_i of 4.7 nM, which has 60-fold higher selectivity compared to trifluoromethyl ketones (Boger et al., 2005). However, OL-135 did not show significant inhibition in vivo, probably due to rapid metabolism (Lichtman et al., 2004). The third group of FAAH inhibitors discovered were N-alkylcarbamates, which are also irreversible inhibitors. The carbamate inhibitor URB597 displays a high inhibitory potency against rat FAAH, with IC₅₀ of 4.6 nM (Mor et al., 2004). The research done on carbamates led to the discovery of the

next generation of FAAH inhibitors containing piperidine urea moiety. This group also inhibits FAAH irreversibly. PF-3845 3, discovered by Pfizer, is one of the most potent inhibitors from this group with the inhibitory potency K_i of 0.23 nM (Ahn, Johnson, Mileni, et al., 2009). There are many other structurally different FAAH inhibitors that we are not able to classify into any aforementioned groups, but are known to be potent FAAH inhibitors, such as boronic acid-based inhibitors, azole derivatives, benzothiazole, and others (Ahn, Johnson, Mileni, et al., 2009; Lodola, Castelli, Mor, & Rivara, 2015; Wang et al., 2009). noticed that the binding pocket of rat FAAH can well-tolerate the big and bulky groups located on the left side of the piperidine series of molecules, while the right side was usually kept small, such as a thiophene group or fluorophenyl groups. In the separate studies (Mor et al., 2008; Tarzia et al., 2003), the synthesis of a series of 2-naphthyl containing carbamates designed as FAAH inhibitors were reported, showing that this bulky, hydrophobic moiety is also important for FAAH inhibition (Figure 2). In both of these studies, the rat FAAH enzyme was used for the biological evaluation of synthesized analogs. Herein, we decided to design, synthesize, and biologically evaluate 2-naphthyl- and 4-phenylthiazole piperidine analogs as potential inhibitors of human FAAH enzyme. Finally, we performed molecular modeling studies to further support and analyze our in vitro data. Our results suggest that 4-phenylthiazole piperidine analogs represent a promising series of FAAH inhibitors with potential therapeutic effects in pain management.

Trifluoromethyl ketone analog of oleamide
$$K_i = 82 \text{ nM}$$

URB597
 $IC_{50} = 4.6 \text{ nM}$

Boronic acid inhibitor

 $IC_{53} = 4.6 \text{ nM}$
 $IC_{50} = 4.6 \text{ nM}$
 IC_{50}

 $IC_{50} = 14 \text{ nM}$

 $IC_{50} = 19 \text{ nM}$

FIGURE 2 Known fatty acid amide hydrolase inhibitors

2 METHODS AND MATERIALS

Reagents and solvents were available from Sigma-Aldrich or Fisher Scientific and used as supplied. All new compounds were characterized by proton NMR, carbon NMR, and high-resolution mass spectrometry. NMR spectra were measured on a Bruker 400 magnetic resonance spectrometer. ¹H chemical shifts are reported relative to the residual solvent peak (chloroform = 7.26 ppm or dimethyl sulfoxide = 2.50 ppm) as follows: chemical shift (δ), proton ID, multiplicity (s = singlet, bs = broad singlet, d = doublet, bd = broad doublet, dd = doublet of doublets, t = triplet, q = quartet, m = multiplet, integration, coupling constant(s)in Hz). ¹³C chemical shifts are reported relative to the residual deuterated solvent ¹³C signals (chloroform = 77.2 ppm, or dimethyl sulfoxide = 39.5 ppm). High-resolution mass spectra were obtained using a high-resolution liquid chromatography mass spectrometer. Microwave reactions were

carried out in a CEM Discover SP microwave synthesizer. Human recombinant FAAH (Item No. 100101183, Batch No. 0523867) was obtained from Cayman Chemical. Molecular modeling studies and docking experiments were performed using ICM PRO MOLSOFT software (Abagyan, Totrov, & Kuznetsov, 1994).

2.1 | Chemistry

The synthesis of 2-naphthyl analogs **8a–c** and 4-phenylthiazole analogs **14a–f** is illustrated in Schemes 1 and 2, respectively. In short, 2-naphthylamine **4** and 1-Bocpiperidine-4-carboxylic acid **5** were coupled under standard EDC-amide coupling conditions to get the amide **6** in 57% yield. The Boc protecting group was subsequently removed using trifluoroacetic acid (TFA). The obtained amine was sulfonated with 2-tiophenesulfonyl chloride,

SCHEME 1 Reagents and conditions: (a) EDC, CH₂Cl₂, rt, 48 hr, 57%; (b) TFA, CH₂Cl₂, rt, 24 hr, 62%: (c) R-sulfonyl chloride, DiPEA, CH₂Cl₂, rt, 24 hr, 38%–86%. Ra: -thiophene-2-yl; Rb: -phenyl; Rc: -2-fluorophenyl

SCHEME 2 Reagents and conditions: (a) iPrOH, 60°C, 2 hr, 90%; (b) EDC, DMAP, CH₂Cl₂, MW irradiation 15 min, 80°C, 53%; (c) TFA, CH₂Cl₂, rt, 24 hr, 94%; (d) Triethylamine, CH₂Cl₂, R-sulfonyl chloride, MW irradiation 20 min, 40%–72%. 14a: 2-tiophenyl; 14b: 2-chlorophenyl; 14c: 2-fluorophenyl; 14d: 4-chlorophenyl; 14e: 4-fluorophenyl; 14f: 2,4-difluorophenyl; 14g: 2,4-dichlorophenyl

benzenesulfonyl chloride, and 2-fluorobenzenesulfonyl chloride to afford analogs 8a, 8b, and 8c, respectively (Pecic, Deng, Morisseau, Hammock, & Landry, 2012). The synthesis of analogs 14a—f started with condensation of commercially available 2-bromoacetophenone 9 and 4-aminothiobenzamide 10. The obtained 4-phenylthiazole aniline 11 was coupled to 1-Boc-piperidine-4-carboxylic 5, using EDC as coupling reagent and microwave irradiation. The Boc group of the resulting amide 12 was removed with TFA to afford the amine 13, which was reacted with various different sulfonyl chlorides to yield the target analogs 14a—f in moderate yields.

2.2 | Human FAAH enzyme inhibition assay

Measurement of FAAH potency was performed using the substrate N-(6-methoxypyridin-3-yl) octanamide (OMP; $[S]_{final} = 50 \,\mu\text{M}$) in sodium phosphate buffer (0.1 M, pH = 8, 0.1 mg/ml BSA), and progress of the reaction was measured at $\lambda_{\text{excitation}} = 303 \,\text{nm}$, $\lambda_{\text{emission}} = 394 \,\text{nm}$, 37°C . All experiments were run in triplicate, and values reported as average \pm SD (Pecic et al., 2018). The substrate OMP was synthesized following synthetic procedure and reaction conditions shown in Scheme 3.

2.3 | Molecular modeling

Amino acid sequence of human FAAH enzyme was retrieved from the NCBI protein database. Sequence alignment was carried out with the ICM Pro (based on ZEGA sequence alignment-Needleman and Wunsch algorithm with zero gap and penalties). To make the homology model, we used a homology algorithm from ICM Pro. Between several crystal structures available in the PDB database, the crystal structure of rat FAAH enzyme (PDB code: 3QK5) was selected as a template. The sequence alignment and the rat FAAH PDB template were converted to the ICM homology model. Conversion included optimization of hydrogens, several amino acids (H, P, N, C, and Q) and assignment of the secondary structure. In order to validate the model, programs Procheck, Verify3D, Errat, What check, and Prove from SAVES metaserver were used. The small molecule docking experiments were performed following steps according to the ICM Pro program guidelines. All synthesized analogs and standard FAAH inhibitor URB-597 were drawn as 2D structures with CHEMDRAW Professional version 16, and then, energy minimized through CHEM3D version 16/MM2, Job Type: Minimum RMS Gradient of 0.010 kcal/mol and RMS distance of 0.1 Å, and saved as MDL MolFiles (*.mol) for purpose of docking with ICM Pro (Pecic et al., 2010, 2018; Pecic, McAnuff, & Harding, 2011). ICM scores were obtained after this procedure. ADME properties for all synthesized target analogs were calculated using the ICM Chemist program.

3 | EXPERIMENTAL

3.1 | General procedure for the preparation of naphthyl analogs 8a-c

tert-butyl 4-(naphthalen-2-ylcarbamoyl)piperidine-1-carboxylate (6): The mixture of N-Boc-piperidinecarboxylic acid 5 (1.01 g, 4.4 mmol) and EDC (1.27 g, 6.6 mmol) was dissolved in anhydrous dichloromethane (45 ml) and was stirred at room temperature. 2-Naphthylamine 4 (756 mg, 5.28 mmol) was slowly added to the reaction mixture and stirred for 48 hr at room temperature under argon atmosphere (Scheme 1). The reaction mixture was transferred to the separatory funnel, and organic layer was washed with 2 N HCl (100 ml), an agueous solution of saturated NaHCO₃ (2×100 ml), and was then dried over anhydrous sodium sulfate. The product was recrystallized with hexane and collected upon filtration. The product 6 was obtained as an off-white solid, 891 mg, 57% yield. ¹H NMR (400 MHz, CDCl₃) δ 8.24 (s, 1H), 7.77 (t, J = 8.4 Hz, 4H), 7.47 - 7.40 (m, 3H), 4.2 (bs, 1H), 2.78 (bs, 1H)2H), 2.45-2.41 (m, 1H), 1.91 (d, J = 14.8 Hz, 2H) 1.81-1.77(m, 2H), 1.49 (s, 9H). 13 C NMR (100 MHz, CDCl₃): δ 173.0, 154.7, 135.2, 133.8, 130.6, 128.7, 127.6, 127.5, 126.5, 125.0, 119.8, 116.8, 79.8, 44.2, 28.4 ppm.

N-(naphthalen-2-yl)piperidine-4-carboxamide (7): The amide 6 (800 mg, 2.25 mmol) was dissolved in anhydrous dichloromethane (25 ml) and was then cooled down to 0°C. TFA (4.32 ml, 56.5 mmol) was slowly added, and the reaction mixture was stirred at 0°C for additional 30 min. Reaction mixture was stirred at room temperature for 48 hr under argon atmosphere. Next, the reaction mixture was concentrated. The crude product was dissolved in ethyl acetate (25 ml), and 10% aqueous solution of NaOH (25 ml) was added slowly and vigorously stirred for 15 min. The mixture was transferred to the separatory funnel, and organic layer was collected, dried over anhydrous sodium

methoxypyridine Octanoic acid

OMP
SCHEME 3 Reagents and conditions:
(a) EDC, CH₂Cl₂, rt, 24 hr, 49%

sulfate, filtered, and concentrated. The product **7** was collected as an off-white solid, 351 mg, 62% yield. ¹H NMR (400 MHz, DMSO- d_6) δ 10.21 (s, 1H), 8.32 (s, 1H), 7.86–7.78 (m, 3H), 7.60 (dd, J=2, 6.8 Hz, 1H), 7.46 (t, J=6.8 Hz, 1H), 7.39 (t, J=8 Hz, 1H), 3.92 (bs, 1H), 3.23 (d, J=12.4 Hz, 2H), 2.80 (t, J=10 Hz, 2H), 2.66–2.59 (m, 1H), 1.89 (d, J=12 Hz, 2H), 1.78–1.70 (m, 2H). ¹³C NMR (100 MHz, DMSO- d_6): δ 173.4, 137.2, 133.8, 130.1, 128.7, 127.8, 127.6, 126.8, 124.9, 120.4, 115.6, 44.0, 41.7, 27.2 ppm.

The amine **7** (50 mg, 0.19 mmol) was dissolved in anhydrous dichloromethane (20 ml), the reaction mixture was brought to 0°C, and N,N-diisopropylethylamine (97 μ L, 0.59 mmol) was added. The reaction mixture was stirred for 30 min, followed by the addition of corresponding benzene-(or 2-thiophene-) sulfonyl chloride (0.30 mmol). The reaction mixture was then stirred at room temperature under argon atmosphere for 48 hr. Next, the reaction was transferred to the separatory funnel where the organic layer was washed with an aqueous solution of saturated NaHCO₃ (50 ml), then dried over anhydrous sodium sulfate, filtered, and concentrated. The crude product was purified by column chromatography (ethyl acetate/hexane 1:1).

N-(naphthalen-2-yl)-1-(thiophen-2-ylsulfonyl)piperidine-4-carboxamide (**8a**) was obtained as an off-white solid in the amount of 30 mg (38% yield): 1 H NMR (400 MHz, DMSO- d_{6}) δ 8.28 (s, 1H), 8.07 (dd, J = 1.2, 4 Hz, 1H), 7.84–7.78 (m, 3H), 7.68 (dd, J = 1.2, 2.4 Hz, 1H), 7.55 (dd, J = 2, 6.8 Hz, 1H), 7.45 (t, J = 7.6 Hz, 1H), 7.38 (t, J = 7.4 Hz, 1H), 7.324–7.30 (m, 1H), 3.68 (d, J = 12 Hz, 2H), 2.46–2.42 (m, 2H), 1.96 (dd, J = 2.8, 10.4 Hz, 2H), 1.78–1.68 (m, 2H). 13 C NMR (100 MHz, DMSO- d_{6}): δ 173.2, 137.1, 135.9, 134.1, 133.8, 133.3, 130.1, 128.7, 127.8, 127.7, 126.8, 124.9, 120.4, 115.6, 45.8, 41.7, 28.0 ppm. HRMS-ESI+: calculated for $C_{20}H_{20}N_{2}O_{3}S_{2}$ + H: 401.0988; Found: 401.0980.

N-(naphthalen-2-yl)-1-(phenylsulfonyl)piperidine-4-carboxamide (**8b**) was obtained as an off-white solid in the amount of 39 mg (50% yield). ¹H NMR (400 MHz, DMSO- d_6) δ 10.02 (s, 1H), 8.27 (s, 1H), 7.84–7.72 (m, 6H), 7.67 (t, J=8 Hz, 2H), 7.54 (d, J=6.8 Hz, 1H), 7.45 (t, J=8 Hz, 1H), 7.38 (t, J=8.4 Hz, 1H), 3.69 (d, J=12 Hz, 2H), 2.39–2.33 (m, 3H), 1.93–1.89 (m, 2H), 1.72–1.64 (m, 2H). ¹³C NMR (100 MHz, DMSO- d_6): δ 173.2, 137.1, 136.0, 133.8, 133.6, 130.1, 129.8, 128.7, 127.8, 127.7, 126.8, 124.9, 120.4, 115.6, 45.8, 41.8, 28.1 ppm. HRMS-ESI+: calculated for C₂₂H₂₂N₂O₃S + H: 395.1424; Found: 395.1416.

1-((2-fluorophenyl)sulfonyl)-*N*-(naphthalen-2-yl)piperidine-4-carboxamide (**8c**) was obtained as a white solid in the amount of 70 mg (86% yield). ¹H NMR (400 MHz, DMSO- d_6) δ 10.08 (s, 1H), 8.29 (s, 1H), 7.84–7.78 (m, 5H), 7.57–7.52 (m, 2H), 7.47 (t, J = 10.6 Hz, 2H), 7.38 (t, J = 6.8 Hz, 1H), 3.76 (d, J = 12 Hz, 2H), 2.66 (t, J = 11.6 Hz, 2H), 1.92 (d, J = 10.4 Hz, 2H), 1.71–1.61 (m, 2H). ¹³C NMR

(100 MHz, DMSO- d_6): δ 173.2, 159.9, 157.4, 137.1, 136.4, 136.3, 133.8, 131.2, 130.1, 128.7, 127.8, 127.7, 126.8, 125.6, 125.3, 125.1, 124.9, 120.4, 118.1, 117.9, 115.7, 45.3, 41.9, 28.2 ppm. HRMS-ESI+: calculated for $C_{22}H_{21}FN_2O_3S + H$: 413.1330; Found: 413.1322.

3.2 | General procedure for the preparation of 4-phenylthiazole analogs 14a-g

The mixture of 2- bromoacetophenone (1.2 g, 6.02 mmol) and 4-aminothiobenzamide (918 mg, 6.02 mmol) was dissolved in isopropanol (25 ml; Scheme 2). The reaction was stirred at 60°C for 2 hr. The reaction mixture was cooled to 0°C, and the crude product was filtered and washed with additional 2 ml cold isopropanol. The crude product, amine **11**, was used for the next step without further purification. **11** was obtained as a dark green solid in the amount of 1.370 g (90% yield). ¹H NMR (400 MHz, DMSO- d_6) δ 8.12 (s, 1H), 8.04–7.98 (m, 4H), 7.47 (t, J = 7.6 Hz, 2H), 7.37 (d, J = 7.2 Hz, 1H), 7.21 (d, J = 8.8 Hz, 2H), 4.44 (bs, 1H). ¹³C NMR (100 MHz, DMSO- d_6): δ 166.5, 154.9, 133.9, 128.8, 128.2, 127.6, 126.1, 120.3, 114.0 ppm.

N-boc-piperidinecarboxylic acid 5 (750 mg, 3.27 mmol), 1-ethyl-3-(3-dimethylaminopropyl) carbodiimide (EDC; 753 mg, 3.92 mmol), amine 11 (825 mg, 3.27 mmol), and catalytic amount of 4-dimethylaminopyridine (DMAP) were dissolved in 20 ml anhydrous dichloromethane. The reaction mixture was subjected to microwave irradiation at 80°C for 15 min. The mixture was transferred to a separatory funnel, and the organic layer was washed with aqueous solution of 1M HCl (20 ml), aqueous solution of saturated NaHCO₃ (20 ml), and brine (20 ml). The organic layer was then dried over anhydrous sodium sulfate, filtered, and concentrated. The crude product was purified by column chromatography (ethyl acetate/hexane 1:1) and 815 mg, 53% of 12 was obtained as a white solid. ¹H NMR (400 MHz, CDCl₃) δ 7.99– 7.96 (m, 3H), 7.62 (d, J = 8.8 Hz, 2H), 7.43 (t, J = 8 Hz, 3H), 7.36-7.32 (m, 1H), 4.18 (bs, 1H), 4.00 (bs, 1H), 2.88-2.75 (m, 2H), 2.51-2.36 (m, 2H), 1.90 (d, J = 12 Hz, 2H), 1.80–1.61 (m, 2H), 1.47 (s, 9H). ¹³C NMR (100 MHz, CDCl₃): δ 179.0, 172.9, 167.3, 156.3, 154.8, 154.8, 139.5, 134.5, 129.9, 128.8, 128.3, 127.5, 126.5, 119.9, 80.0, 44.4, 40.8, 28.5, 27.9 ppm.

The amide **12** (792 mg, 1.71 mmol) was dissolved in anhydrous dichloromethane (20 ml), and reaction mixture was cooled down to 0°C. TFA (2.62 ml, 34.2 mmol) was added slowly, and the reaction mixture was stirred at room temperature for 24 hr under argon atmosphere. Solvents were evaporated, and the crude product was recrystallized from diethyl ether, and 685 mg (94% yield) was obtained as a TFA salt. A small amount of product was freebased and used for 1 H and 13 C NMR analysis. 1 H NMR (400 MHz, DMSO- d_{6}) δ

10.13 (s, 1H), 8.10 (s, 1H), 8.05 (d, J = 7.2 Hz, 2H), 7.97 (d, J = 8.8 Hz, 2H), 7.78 (d, J = 8.8 Hz, 2H), 7.47 (t, J = 7.2 Hz, 2H), 7.37 (t, J = 7.6 Hz, 1H), 3.01 (d, J = 11.6 Hz, 2H), 2.55–2.53 (m, 1H), 1.72 (d, J = 10.8 Hz, 2H), 1.60–1.50 (m, 2H). ¹³C NMR (100 MHz, DMSO- d_6): δ 173.9, 166.8, 154.9, 141.3, 134.0, 128.7, 128.1, 127.6, 126.8, 126.1, 119.2, 113.8, 45.3, 43.4, 29.0 ppm.

The amine 13 (100 mg, 0.209 mmol) was dissolved in 20 ml of anhydrous dichloromethane and triethylamine (0.2 ml, 1.045 mmol) was added, followed by addition of corresponding benzene- (or 2-thiophene-) sulfonyl chloride (0.314 mmol) and was subjected to microwave irradiation at 80°C for 15 min. The reaction mixture was then transferred to the separatory funnel, and the organic layer was washed with 30 ml of an aqueous solution of saturated sodium bicarbonate, dried over anhydrous sodium sulfate, and then concentrated. The final 4-phenylthiazole analogs were purified by column chromatography (ethyl acetate/hexane 1:4).

N-(4-(4-phenylthiazol-2-yl)phenyl)-1-(thiophen-2-ylsulfonyl)piperidine-4-carboxamide (**14a**) was obtained as an white solid in the amount of 54 mg (50% yield): 1 H NMR (400 MHz, DMSO- d_6) δ 10.12 (s, 1H), 8.11 (s, 1H), 8.07–8.03 (m, 3H), 7.96 (d, J = 8.8 Hz, 2H), 7.74 (d, J = 8.8 Hz, 2H), 7.68–7.67 (m, 1H), 7.47 (t, J = 7.6 Hz, 2H), 7.35 (d, J = 12.8 Hz, 1H), 7.30 (t, J = 3.6 Hz, 1H), 3.68 (d, J = 12 Hz, 2H), 2.47–2.40 (m, 3H), 1.92 (d, J = 13.6 Hz, 2H), 1.75–1.65 (m, 2H). 13 C NMR (100 MHz, DMSO- d_6): δ 173.0, 166.9, 155.1, 141.2, 135.6, 134.2, 133.9, 133.1, 128.9, 128.5, 128.3, 128.0, 127.0, 126.3, 119.5, 114.0, 45.5, 41.5, 27.6 ppm. HRMS-ESI+: calculated for $C_{25}H_{23}N_3O_3S_3$ + H: 510.0974; Found: 510.0962.

1-((2-fluorophenyl)sulfonyl)-*N*-(4-(4-phenylthiazol-2-yl) phenyl)piperidine-4-carboxamide (**14b**) was obtained as an white solid in the amount of 44 mg (40% yield). ¹H NMR (400 MHz, DMSO- d_6) δ 10.14 (s, 1H), 8.10 (s, 1H), 8.03 (d, J=7.2 Hz, 2H), 7.96 (d, J=8 Hz, 2H), 7.83–7.73 (m, 4H), 7.54–7.43 (m, 2H), 7.36 (t, J=7.2 Hz, 1H), 3.75 (d, J=12.4 Hz, 2H), 2.65 (t, J=11.6 Hz, 2H), 1.91 (d, J=10.4 Hz, 2H), 1.68–1.60 (m, 2H). ¹³C NMR (100 MHz, DMSO- d_6): 173.0, 166.9, 155.1, 141.2, 136.1, 136.0, 134.2, 131.0, 128.9, 128.3, 128.0, 127.0, 126.2, 125.4, 125.3, 125.0, 119.5, 117.8, 117.6, 114.0, 45.0, 41.6, 27.9 ppm. HRMS-ESI+: calculated for C₂₇H₂₄FN₃O₃S₂ + H: 522.1316; Found: 522.1302.

1-((2-chlorophenyl)sulfonyl)-*N*-(4-(4-phenylthiazol-2-yl) phenyl)piperidine-4-carboxamide (**14c**) was obtained as an off-white solid in the amount of 62.1 mg (55% yield). ¹H NMR (400 MHz, DMSO- d_6) δ 10.19 (s, 1H), 8.10 (s, 1H), 8.05–7.95 (m, 5H), 7.76–7.67 (m, 4H), 7.58 (t, J = 8 Hz, 1H), 7.47 (t, J = 7.6 Hz, 2H), 7.37 (t, J = 7.6 Hz, 1H), 3.78 (d, J = 12.8 Hz, 2H), 2.84 (t, J = 12.4 Hz, 2H), 2.55–2.51 (m, 1H), 1.89 (d, J = 10.8 Hz, 2H), 1.62 (dd, J = 11.6, 9.2 Hz,

2H). 13 C NMR (100 MHz, DMSO- d_6): δ 172.9, 166.7, 154.9, 141.0, 135.8, 134.4, 134.0, 132.2, 131.5, 130.8, 128.8, 128.7, 128.1, 127.8, 126.8, 126.0, 119.3, 113.8, 44.7, 41.7, 28.0 ppm. HRMS-ESI+: calculated for $C_{27}H_{24}ClN_3O_3S_2 + H$: 538.1020; Found: 538.1007.

1-((4-fluorophenyl)sulfonyl)-*N*-(4-(4-phenylthiazol-2-yl) phenyl)piperidine-4-carboxamide (**14d**) was obtained as white solid in the amount of 79 mg (72% yield). ¹H NMR (400 MHz, DMSO- d_6) δ 10.09 (s, 1H), 8.09 (s, 1H), 8.03 (d, J=7.2 Hz, 2H), 7.96 (d, J=8.8 Hz, 2H), 7.87–7.83 (m, 2H), 7.73 (d, J=8.8 Hz, 2H), 7.52–7.44 (m, 4H), 7.36 (t, J=7.6 Hz, 1H), 3.68 (d, J=12 Hz, 2H), 2.36 (t, J=11.6 Hz, 3H), 1.89 (d, J=10.4 Hz, 2H), 1.70–1.62 (m, 2H). ¹³C NMR (100 MHz, DMSO- d_6): δ 172.8, 166.7, 154.9, 141.0, 134.0, 132.1, 132.0, 130.5, 130.4, 128.7, 128.1, 127.8, 126.8, 126.0, 119.3, 116.7, 116.4, 113.8, 45.2, 41.4, 27.5 ppm. HRMS-ESI+: calculated for $C_{27}H_{24}FN_3O_3S_2 + H$: 522.1316; Found: 522.1302.

1-((4-chlorophenyl)sulfonyl)-*N*-(4-(4-phenylthiazol-2-yl) phenyl)piperidine-4-carboxamide (**14e**) was obtained as a white solid, 59 mg (53% yield). ¹H NMR (400 MHz, DMSO- d_6) δ 10.12 (s, 1H), 8.09 (s, 1H), 8.03 (d, J=7.2 Hz, 2H), 7.95 (d, J=8.8 Hz, 2H), 7.80–7.77 (m, 2H), 7.73 (d, J=8.8 Hz, 4H), 7.46 (t, J=7.2 Hz, 2H), 7.36 (d, J=7.2 Hz, 1H), 3.68 (d, J=12 Hz, 2H), 2.42–2.35 (m, 3H), 1.89 (d, J=10.8 Hz, 2H), 1.71–1.61 (m, 2H). ¹³C NMR (100 MHz, DMSO- d_6): δ 172.8, 166.7, 154.9, 141.0, 138.1, 134.6, 134.0, 129.5, 129.3, 128.7, 128.1, 127.8, 126.8, 126.1, 119.3, 113.8, 45.2, 41.3, 28.0, 27.5 ppm. HRMS-ESI+: calculated for $C_{27}H_{24}ClN_3O_3S_2 + H$: 538.1020; Found: 538.1006.

1-((2,4-difluorophenyl)sulfonyl)-N-(4-(4-phenylthiazol-2-yl)phenyl)piperidine-4-carboxamide (**14f**) was obtained as off-white solid, 46 mg (41% yield). ¹H NMR (400 MHz, DMSO- d_6) δ 10.15 (s, 1H), 8.10 (s, 1H), 8.04 (d, J = 7.2 Hz, 2H), 7.96 (d, J = 8.8 Hz, 2H), 7.92–7.86 (m, 1H), 7.74 (d, J = 9.2 Hz, 2H), 7.66–7.61 (m, 1H), 7.47 (t, J = 7.2 Hz, 2H), 7.38–7.32 (m, 2H), 3.73 (d, J = 12.4 Hz, 2H), 2.66 (t, J = 11.6 Hz, 2H), 1.91 (d, J = 10.4 Hz, 2H), 1.69–1.59 (m, 2H). ¹³C NMR (100 MHz, DMSO- d_6): δ 173.0, 166.9, 155.1, 141.2, 134.2, 133.1, 128.9, 128.3, 128.0, 127.0, 126.2, 119.5, 114.0, 112.8, 106.5, 44.9, 41.6, 27.9 ppm. HRMS-ESI+: calculated for $C_{27}H_{23}F_2N_3O_3S_2 + H$: 540.1222; Found: 540.1205.

1-((2,4-dichlorophenyl)sulfonyl)-*N*-(4-(4-phenylthiazol-2-yl)phenyl)piperidine-4-carboxamide (**14g**) was obtained as an pale yellow solid in the amount of 93 mg (68% yield). ¹H NMR (400 MHz, DMSO- d_6) δ 10.19 (s, 1H), 8.10 (s, 1H), 8.05–7.94 (m, 6H), 7.75 (d, J=8.8 Hz, 2H), 7.67 (d, J=10.8 Hz, 1H), 7.47 (t, J=7.6 Hz, 2H), 7.37 (t, J=7.6 Hz, 1H), 3.77 (d, J=12.8 Hz, 2H), 2.86 (t, J=12 Hz, 2H), 2.55–2.51 (m, 1H), 1.89 (d, J=10.8 Hz, 2H), 1.62 (dd, J=12, 8.8 Hz, 2H). ¹³C NMR (100 MHz, DMSO- d_6): δ 172.8, 166.7, 154.9, 141.0, 138.4, 134.9, 134.0,

132.8, 132.2, 131.7, 128.7, 128.1, 127.9, 127.8, 126.8, 126.0, 119.3, 113.8, 44.7, 41.6, 28.0 ppm. HRMS-ESI+: calculated for $C_{27}H_{23}Cl_2N_3O_3S_2 + H$: 572.3428; Found: 572.0631.

3.3 | OMP synthesis

A mixture of octanoic acid (350 mg, 2.43 mmol), 5-Amino-2-methoxypyridine (302 mg, 2.43 mmol), and EDC (700 mg, 3.65 mmol) was dissolved in anhydrous DCM (20 ml) and stirred overnight (Scheme 3). The mixture was transferred to separatory funnel, washed with aqueous solution of 1M HCl (200 ml), followed by an aqueous solution of saturated sodium bicarbonate, the organic layer was dried over anhydrous sodium sulfate, filtered, and concentrated. The crude OMP was purified by column chromatography (ethyl acetate/hexane 1:4). The product (301 mg, 49% yield) was obtained as a pale yellow solid.

N-(6-methoxypyridin-3-yl) octanamide (OMP): ¹H NMR (400 MHz, CDCl₃) δ 8.14 (s, 1H), 7.90 (dd, J = 2.8, 6.4 Hz, 1H), 7.51 (s, 1H), 6.71 (d, J = 8.8 Hz, 1H), 3.91 (s, 3H), 2.35 (t, J = 7.2 Hz, 2H), 1.71 (t, J = 6.8 Hz, 2H), 1.29–1.28 (m, 8H), 0.88 (t, J = 6.8 Hz, 3H). ¹³C NMR (100 MHz, CDCl₃): δ 171.9, 160.9, 138.6, 132.4, 128.6, 110.5, 53.5, 37.3, 31.6, 29.2, 29.0, 25.6, 22.5, 14.0 ppm. HRMS-ESI+: calculated for $C_{14}H_{23}N_2O_2$ + H: 251.1760; Found: 251.1749.

4 | RESULTS AND DISCUSSION

4.1 Design, synthesis, and SAR

In previous studies (Figure 3), Wang et al. (2009) examined various benzothiazole and 4-phenylthiazole piperidine moieties identified from high-throughput screening and follow-up structure–activity relationship (SAR) studies. This study mostly focused on the benzothiazole–piperidine analogs and reported only three analogs with various 4-phenylthiazole groups on the left side of the piperidine series of analogs.

Mor et al. (2008) reported two potent 2-naphthyl containing FAAH inhibitors. We hypothesized that the FAAH inhibitory activity may be achieved by introducing the 2-naphthyl ring into piperidine series of analogs. Our design started with introducing 2-naphthyl ring on the left side of the piperidine moiety and linking the small thiophene, phenyl or 2-fluorophenyl rings on the right side of the central piperidine moiety via sulfonamide bond. Our docking experiments (Table 1) suggested that this series of bulky, hydrophobic naphthyl analogs fits well in the binding pocket of the human FAAH, according to the obtained low ICM scores. The first tested 2-naphthyl-piperidine analog 8a showed only weak submicromolar potency with IC₅₀ of 1,700 nM. Replacing the thiophene ring with other small rings, such as phenyl 8b, or 2-fluorophenyl 8c, did not improve the inhibitory activity of this series of analogs, as shown in Table 1, with IC₅₀s of 4,500 and 1,200 nM, respectively, indicating that 4-phenylthiazole moiety is the important structural feature on the piperidine series of FAAH inhibitors. We decided to turn our attention to the 4-phenylthiazole analogs, as this moiety showed improved potency and was not well-explored in previous studies, namely only three analogs were synthesized and evaluated in rat FAAH inhibition assay (Figure 3). In addition, 4-phenylthiazole without any substitution on the phenyl ring was never tested, and our docking experiments suggested that this moiety will occupy the same hydrophobic pocket as the other bulky, hydrophobic groups previously reported. In order to explore the structural requirements for this series of analogs, we prepared several compounds containing 4-phenylthiazole moiety without any substituents on the phenyl ring on the left side of the piperidine ring, and fluorine and chlorine atoms at various positions on the aromatic ring on the right side of the molecule and evaluated these analogs for inhibition against human FAAH enzyme. Biological evaluation of the first 4-phenylthiazole analog 14a, containing a thiophene ring on the right side of the piperidine moiety, showed very good inhibitory potency against human FAAH enzyme with IC₅₀ of 23.4 nM. We continued our SAR exploration of the 4-phenylthiazole analogs with probing

FIGURE 3 Design of new series of fatty acid amide hydrolase inhibitors

8a-c Analogs

14a-g Analogs



TABLE 1 Fatty acid amide hydrolase (FAAH) inhibitory activity and docking scores of analogs

| Compound | FAAH IC ₅₀ (nM) | Docking score |
|----------|----------------------------|---------------|
| URB-597 | 38 | -21.45 |
| 8a | 1,700 | -32.73 |
| 8b | 4,500 | -29.11 |
| 8c | 1,200 | -29.9 |
| 14a | 23.4 | -25.87 |
| 14b | 19.5 | -22.34 |
| 14c | 30.8 | -23.16 |
| 14d | 9.6 | -27.78 |
| 14e | 54 | -21.46 |
| 14f | 8.4 | -31.75 |
| 14g | 11.9 | -25.01 |

the 2-fluorophenyl **14b**, 2-chlorophenyl **14c**, 4-fluorophenyl **14d**, 4-chlorophenyl **14e**, 2,4-difluorophenyl **14f**, and 2,4-dichlorophenyl **14g** groups on the right side of the 4-phenylthiazole piperidine moiety. All analogs showed improved potencies, having IC₅₀s in the low-to-medium nanomolar range, and also suggesting that *ortho*- and *para*-substituted and *ortho-para* disubstituted fluorine atoms are better tolerated than the chlorines at the same positions on the ring. In addition, the improved potencies in the binding pocket of the human FAAH are suggesting potential favorable interactions within the enzyme binding pocket, which were confirmed by our docking experiments.

4.2 | Homology modeling studies

In order to better explore the possible binding modes and interactions for the 4-phenylthiazole analogs, we have conducted molecular modeling studies. As the crystal structure of the human FAAH enzyme has not been reported, we decided to build a homology model. As a template for building the human FAAH enzyme homology model, we selected the crystal structure of the rat FAAH (PDB code: 3QK5) (Gustin et al., 2011) as its crystal structure is solved at the highest resolution (2.20 Å) that we found deposited. The sequence alignment of the human FAAH enzyme shows very good sequence identity with rat (and many other species) FAAH enzyme sequence template, with 80% sequence similarity (see Figures S1 and S2). We also noticed that the alignment of rat and human FAAH sequences contains many conserved residues (shown by green), especially located in the proximity of the catalytic site of the FAAH enzyme, that are essential for proper enzyme function. We first built and energy minimized the homology model using ICM Pro program, and then, we assessed validity of the model. In order to evaluate the constructed human FAAH enzyme homology model

for the docking studies, we used several different programs for evaluation that are available via the server of the UCLA-DOE Institute for Genomics and Proteomics. Evaluation methods verify whether a model satisfies standard and geometric criteria and asses the overall quality of the model. We used PROCHECK (Laskowski, Rullmann, MacArthur, Kaptein, & Thornton, 1996), ERRAT (Colovos & Yeates, 1993), VERIFY-3D (Eisenberg, Lüthy, & Bowie, 1997), WHAT-IF (Vriend & Sander, 1993), and PROVE (Pontius, Richelle, & Wodak, 1996) and assessed the quality of the human FAAH enzyme model we constructed. We first determined the root-mean-square deviation (RMSD) between the backbone atoms of the template and the homology model, getting RMSD value of 0.238 Å, indicating a close homology (Figure S3). Therefore, we decided to proceed with the next evaluation steps. We then evaluated our homology model using the program Procheck. The aim of this program is to assess the detailed residue-by-residue stereochemical quality of the enzyme structure. Ramachandran plots for the human FAAH homology model are shown in Figure S4. A simple measure of quality that can be used from the plot is the percentage of residues in core region, and allowed regions should be very high (>90% residues). Another important factor in structural assessment is Goodness factor or G-Factor which shows the quality of dihedral, covalent, and overall bond angles. These scores should be above -0.5 for a reliable model. From observing the Ramachandran plot, it can be seen that 89.1% of the residues are in the most favorable region. In addition, 10.5% of the residues were found in the additionally allowed region. To add on, the model was found to have a Gfactor of 0.2, meaning the quality of the bond angles indicates the high quality of our homology model. The results obtained from Errat are shown in Figure S5. This program evaluates an overall quality factor of nonbonded atomic interactions. The normally accepted range is above 50% for a high-quality model. The template structure of rat FAAH enzyme, PDB: 3QK5, has an Errat value of 85.294. From running an Errat on the FAAH homology model, it was found to have an overall quality factor of 93.585, suggesting the backbone conformation and nonbonded interactions of the homology model are all within a normal range. Verify3D evaluates energetic and empirical methods to produce averaged data points for each residue in order to evaluate the quality of protein structures. Verify3D results shown in Figure S6 represent the Verify3D average data score of the homology model generated in comparison with template. Using this scoring function, if more than 80% of the residue has scored above 0.2, then the structure is considered high quality. From the data collected in the table, it was observed that 92.65% of the residues had averaged a 3D score above 0.2. WHAT-IF is used to check the normality of the local environment of amino acids. The program evaluates the following: bond lengths, bond angles, omega angle restraints, side-chain planarity, improper dihedral distribution, and inside/outside distribution. It does extensive checking of many stereochemical parameters of the residues in the model and it gives an overall summary of the quality of the structure as compared with current reliable structures. For a reliable structure, the WHAT-IF packing scores should be above -5.0. In the case of our homology model (Table S1), the packing score is -0.794; therefore, the WHAT-IF evaluation also indicates that the homology model structure is very reasonable.

The Prove results for the human FAAH homology model are shown in Figure S7. Prove provides an average volume Z-score of all the atoms. High scores have been found to be associated with uncertainty in the structure. Structures with poor resolution generally have a Z-score RMS >1.2; while for well-resolved structures, the Z-score RMS is around 1.0 (Pontius et al., 1996). Our model showed that the average Zscore for the model for all resolutions hovered slightly above 0 but below 0.1 with the exception of one outlier at about 0.8. The Prove score shows that the model is valid, but it contains an unusual number of buried atoms within it. The buried atoms are most likely hydrophobic residues within the enzyme. In summary, the geometric quality of the backbone conformation, the residue interaction, the residue contacts, and the energy profile of the human FAAH homology model are all well within the limits established for reliable structure and we proceeded with the docking experiments.

4.3 | Docking experiments

In order to better understand the binding modes and interactions of these inhibitors within the catalytic site of the human FAAH enzyme, we performed docking studies. Scoring functions from this docking experiment are reported in Table 1. The known irreversible FAAH inhibitor URB-597 (1) was also docked for comparison. Although the docking scores for the naphthyl analogs 8a-c had reasonable ICM scores, we were not able to correlate these values with the obtained IC₅₀ values. On the other hand, the docking scores for URB-597 and for the potent 4-phenylthiazole analogs 14a-g were in the agreement with our in vitro data, suggesting that our homology model could be an important tool in the future design for the 4-phenylthiazole series of FAAH inhibitors. After visual inspections of binding modes of these inhibitors, we observed that several inhibitors formed a complex with the FAAH enzyme through H-bonding with different amino acids. All other non-covalent interactions (listed in Table 2) were also located in the proximity of the catalytic triad of the human FAAH enzyme, suggesting that the low nanomolar potency of these compounds is probably due to these interactions. In addition, we also observed that the 4-phenylthiazole moiety was orientated toward the enzyme surface and that the right side of analogs 14b, 14c, 14e, 14f, and 14g is deeply buried within the catalytic site. Figures 4 and 5 show the observed orientation for the most potent fluoro- and chloro-analogs 14f and 14g, respectively. This could also rationalize the differences in the observed IC50 values of this series of inhibitors (see Figures S8–S12). According to the list of the non-covalent interactions (Table 2), all synthesized 4-phenylthiazole analogs are located in the proximity of the catalytic triad residues S217 and S241. We believe that 4-phenylthiazole analogs probably form a non-covalent complex with Ser241 and S217, similar to the intermediate formed by FAAH and anandamide (Figure 1b) during the mechanism of hydrolysis.

TABLE 2 The list of non-covalent interactions of 4-phenylthiazole series of analogs

| Compound | H-bonds | Hydrophobic interactions | Other non-covalent interactions |
|----------|------------|--|---|
| 14a | L401, G485 | F192, S193, Y194, I238, G239, G240, S241, F244, F381, L404, I407, V422, L429, L433, M436, T488, V491, W531 | M191, G402, D403, F432 |
| 14b | 0 | F192, S193, Y194, G239, G240, S241, F244, F381, D403, L404, I407, V422, L429, L433, G485, T488, V491, I530, W531 | M191, G216, S217, L380, L401, M495 |
| 14c | 0 | F192, S193, Y194, I238, G239, G240, S241, F244, D403, L404, I407, V422, L429, L433, M436, T488, V491, I530, W531 | M191, G216, S217, L380, L401, G485, M495 |
| 14d | 0 | F192, S193, Y194, S217, G239, S241, F244, L380, F381, L404, I407, L429, F432, L433, M436, T488, V491, I530, W531 | M191, G216, G240 |
| 14e | T488 | M191, F192, S193, Y194, I238, G239, D403, L404, I407, V422, L429, L433, M436, I530, W531 | S241, F244, L401, G485, V491 |
| 14f | G485, S241 | M191, F192, S193, Y194, I238, G239, L380, L404, I407, V422, L429, F432, L433, M436, T488, V491, I530, W531 | S217, F244 |
| 14g | 0 | F192, S193, Y194, G239, G240, S241, F244, L404, I407, V422, L429, F432, L433, M436, G485, T488, V491, M495, I530, W531 | G216, S217, F381, L401, P484 |
| URB-597 | G272, C269 | F192, I238, K263, L266, G268, Y271, E274, R277, L278 | L154, S190, M191, K267, C269, V270, Q273 |

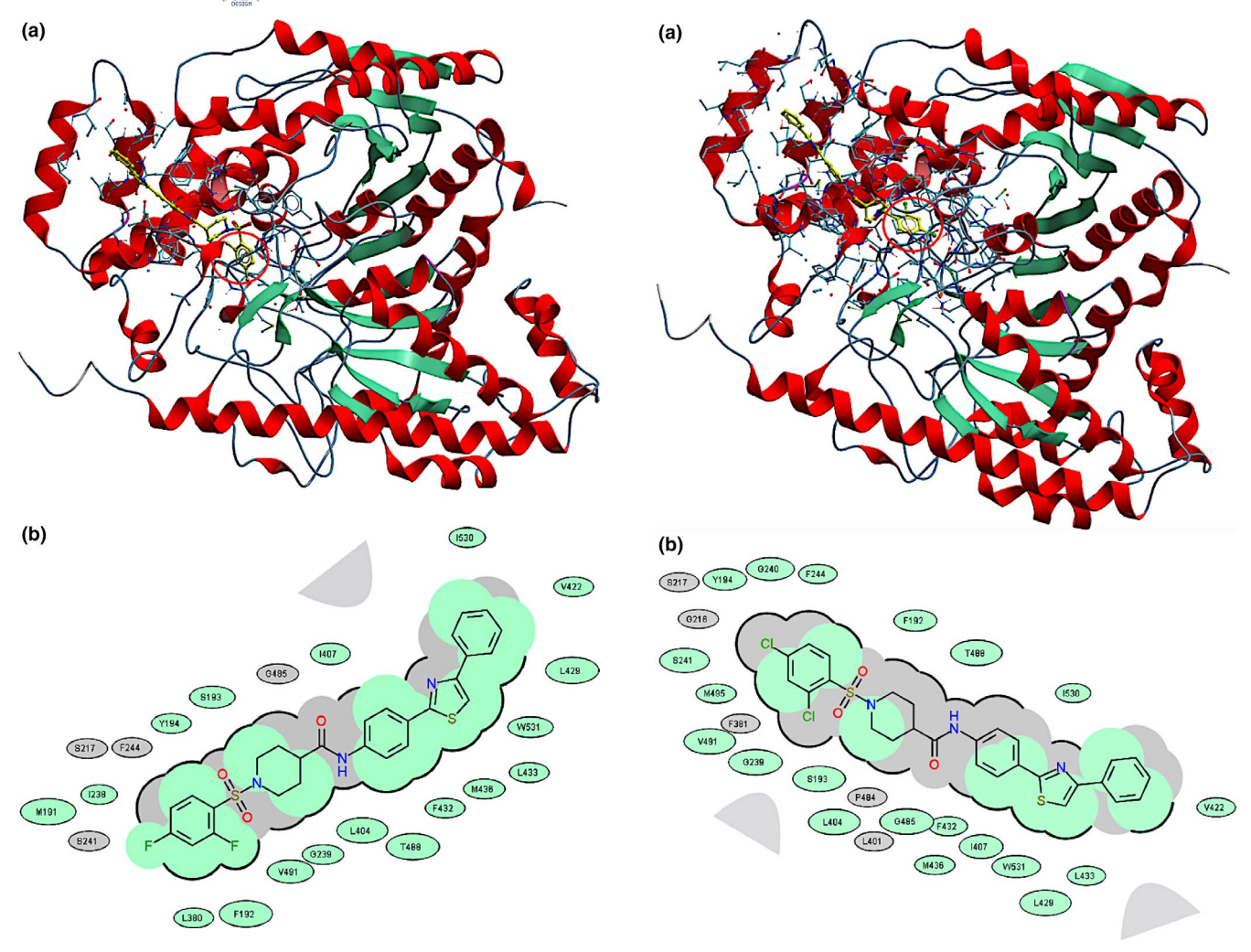


FIGURE 4 (a) A docking pose of the inhibitor 14f in the catalytic site of the human fatty acid amide hydrolase (FAAH) enzyme, suggesting that 2,4-difluorophenyl part (circled in red) of the inhibitor is orientated within the binding pocket. (b) 2D representation for the lowest energy conformation of inhibitor 14f in the binding pocket of human FAAH. Green shading represents hydrophobic region; gray parabolas represent accessible surface for large areas; broken thick line around ligand shape indicates accessible surface; size of residue ellipse represents the strength of the contact [Colour figure can be viewed at wileyonlinelibrary.com]

We also observed potential π - π interactions between F192 and the phenyl aromatic ring of the analogs **14d**, **14f**, and **14g** which could rationalize the improved potencies of these analogs.

4.4 | Predicting ADME-Tox properties

Finally, we calculated and performed prediction of the several pharmacokinetic parameters important for the drug development process, Table 3. All final compounds showed predicted octanol/water partition coefficient (*clogP*) in the relatively acceptable range (2.0–6.5 is considered a good

FIGURE 5 (a) A docking pose of the inhibitor 14g in the catalytic site of the human fatty acid amide hydrolase (FAAH) enzyme, showing that 2,4-dichlorophenyl moiety (circled in red) is located deeply in the binding pocket of the human FAAH enzyme. (b) 2D representation for the lowest energy conformation of inhibitor 14g in the binding pocket of human FAAH. Green shading represents hydrophobic region; gray parabolas represent accessible surface for large areas; broken thick line around ligand shape indicates accessible surface; size of residue ellipse represents the strength of the contact [Colour figure can be viewed at wileyonlinelibrary.com]

logP), moderate predicted aqueous solubility (acceptable range for logS is between -6.5 and -0.5 moles/liter) and no unwanted or reactive chemical functionalities (referred as "bad groups" in the table). Other predicted values that we examined were all within optimum ranges: hydrogen bond donors, hydrogen bond acceptors, and overall drug likeness, which should be within -1 and 1 range. Predicted *Caco2* permeability indicates high permeability (all values above -5 suggest a high permeability), and this series of analogs had excellent predicted values for *hERG* inhibition, namely values above 0.5 indicate high probability for drug candidate of being a *hERG* inhibitor. All final compounds (except standard URB-597) had values below 0.5.

Predicted ADME-Tox properties of synthesized analogs

TABLE 3

Tox score 1.242 1.242 1.242 0 0 0 hERG inhibition 0.149 0.255 0.182 0.209 0.342 0.371 0.31 0.31 Half-life (hr) 1.083 2.048 2.048 1.839 1.839 3.264 2.264 1.531 -5.148-5.135 -5.163-5.207 -4.985-5.053 -5.177-5.168-5.263# of H-B donors acceptors ∞ ∞ ∞ ∞ # of Rot bonds Bad groups 0 0 0 0 0 0 0 Drug likeness 0.015 1.008 -0.0330.714 0.666 0.807 1.223 0.707 -0.081-6.836 -9.159-9.103-6.359-9.062-9.543-9.268-10.085-6.168**cLogP** 4.573 5.785 6.003 6.448 4.022 4.355 4.424 6.123 6.568 6.273 Mol. Wt. 521.1243 521.1243 539.1148 400.0915 394.1351 412.1257 509.0901 537.0947 537.0947 338.163 Compound URB-597 14b 14c 14d **14f** 8c

Our further prediction of plasma half-life showed that these compounds have a moderate predicted half-life of 1.05–3.75 hr. In addition, all newly synthesized 4-phenylthiazole analogs had no unfavorable substructure/substituents, shown as a *tox score* of 0.

5 | CONCLUSIONS

We successfully synthesized 10 new compounds using microwave irradiation and evaluated them in inhibition assay against human FAAH enzyme. Biological evaluation of the two different groups of inhibitors showed that 4-phenylthiazole moiety is an important structural feature for the potent inhibition of human FAAH enzyme and we identified several inhibitors in the low nanomolar range. Using homology modeling and docking studies, we further explored the binding modes of the potent analogs and we noticed several important non-covalent interactions that contribute to the low nanomolar potency of this series of inhibitors. Our calculation of predicted ADME-Tox properties suggests that 4-phenylthiazole inhibitors have the potential to be further developed as new lead candidates and therapeutics in pain management.

ACKNOWLEDGMENTS

This research was financially supported by startup funds granted by the College of Natural Sciences and Mathematics at California State University, Fullerton and Project RAISE, U.S. Department of Education HSI-STEM award number P031C160152. Instrumentation support was provided by the National Science Foundation MRI (CHE1726903) for acquisition of an UPLC-MS.

CONFLICT OF INTEREST

The authors declare that there is no conflict of interest regarding the publication of this article.

DATA AVAILABILITY STATEMENT

The data that support the findings of this study are available from the corresponding author upon reasonable request.

ORCID

Stephanie R. Wilt https://orcid. org/0000-0002-4898-0250 Stevan Pecic https://orcid.org/0000-0002-3706-8768

REFERENCES

Abagyan, R., Totrov, M., & Kuznetsov, D. (1994). ICM—A new method for protein modeling and design: applications to docking and structure prediction from the distorted native conformation. *Journal of Computational Chemistry*, 15(5), 488–506. https://doi.org/10.1002/ jcc.540150503

- Ahn, K., Johnson, D. S., & Cravatt, B. F. (2009). Fatty acid amide hydrolase as a potential therapeutic target for the treatment of pain and CNS disorders. *Expert Opinion on Drug Discovery*, *4*(7), 763–784. https://doi.org/10.1517/17460440903018857
- Ahn, K., Johnson, D. S., Mileni, M., Beidler, D., Long, J. Z., McKinney, M. K., ... Cravatt, B. F. (2009). Discovery and characterization of a highly selective FAAH inhibitor that reduces inflammatory pain. *Chemistry and Biology*, 16(4), 411–420. https://doi.org/10.1016/j.chembiol.2009.02.013
- Basavarajappa, B. S. (2017). Cannabinoid receptors and their signaling mechanisms. In E. Murillo-Rodríguez (Ed.), *The endocannabinoid system* (pp. 25–62). Cambridge, MA: Academic Press.
- Bisogno, T., & Maccarrone, M. (2013). Latest advances in the discovery of fatty acid amide hydrolase inhibitors. *Expert Opinion on Drug Discovery*, 8(5), 509–522. https://doi.org/10.1517/17460 441.2013.780021
- Boger, D. L., Miyauchi, H., Du, W., Hardouin, C., Fecik, R. A., Cheng, H., ... Cravatt, B. F. (2005). Discovery of a potent, selective, and efficacious class of reversible α-ketoheterocycle inhibitors of fatty acid amide hydrolase effective as analgesics. *Journal of Medicinal Chemistry*, 48(6), 1849–1856. https://doi.org/10.1021/jm049614v
- Boger, D. L., Sato, H., Lerner, A. E., Austin, B. J., Patterson, J. E., Patricelli, M. P., & Cravatt, B. F. (1999). Trifluoromethyl ketone inhibitors of fatty acid amide hydrolase: A probe of structural and conformational features contributing to inhibition. *Bioorganic* and Medicinal Chemistry Letters, 9(2), 265–270. https://doi. org/10.1016/s0960-894x(98)00734-3
- Colovos, C., & Yeates, T. O. (1993). Verification of protein structures: Patterns of nonbonded atomic interactions. *Protein Science*, 2(9), 1511–1519. https://doi.org/10.1002/pro.5560020916
- Davis, M. P. (2014). Cannabinoids in pain management: CB1, CB2 and non-classic receptor ligands. Expert Opinion on Investigational Drugs, 23(8), 1123–1140. https://doi.org/10.1517/13543 784.2014.918603
- Eisenberg, D., Lüthy, R., & Bowie, J. U. (1997). VERIFY3D: Assessment of protein models with three-dimensional profiles. *Methods in Enzymology*, 277, 396–404. https://doi.org/10.1016/s0076-6879(97)77022-8
- Gustin, D. J., Ma, Z., Min, X., Li, Y., Hedberg, C., Guimaraes, C., ... Kayser, F. (2011). Identification of potent, noncovalent fatty acid amide hydrolase (FAAH) inhibitors. *Bioorganic and Medicinal Chemistry Letters*, 21(8), 2492–2496. https://doi.org/10.1016/j. bmcl.2011.02.052
- Hruba, L., & McMahon, L. R. (2017). Apparent affinity estimates and reversal of the effects of synthetic Cannabinoids AM-2201, CP-47,497, JWH-122, and JWH-250 by rimonabant in Rhesus Monkeys. *Journal of Pharmacology and Experimental Therapeutics*, 362(2), 278–286. https://doi.org/10.1124/jpet.117.240572
- Laskowski, R. A., Rullmann, J. A. C., MacArthur, M. W., Kaptein, R., & Thornton, J. M. (1996). AQUA and PROCHECK-NMR: Programs for checking the quality of protein structures solved by. *Journal of Biomolecular NMR*, 8(4), 477–486. https://doi.org/10.1007/bf002 28148
- Le Boisselier, R., Alexandre, J., Lelong-Boulouard, V., & Debruyne, D. (2017). Focus on cannabinoids and synthetic cannabinoids. *Clinical Pharmacology and Therapeutics*, 101(2), 220–229. https://doi.org/10.1002/cpt.563
- Lichtman, A. H., Leung, D., Shelton, C. C., Saghatelian, A., Hardouin, C., Boger, D. L., & Cravatt, B. F. (2004). Reversible inhibitors of fatty acid amide hydrolase that promote analgesia: Evidence for an

- unprecedented combination of potency and selectivity. *Journal of Pharmacology and Experimental Therapeutics*, 311(2), 441–448. https://doi.org/10.1124/jpet.104.069401
- Lodola, A., Castelli, R., Mor, M., & Rivara, S. (2015). Fatty acid amide hydrolase inhibitors: A patent review (2009–2014). Expert Opinion on Therapeutic Patents, 25(11), 1247–1266. https://doi. org/10.1517/13543776.2015.1067683
- Lu, Y., & Anderson, H. D. (2017). Cannabinoid signaling in health and disease. Canadian Journal of Physiology and Pharmacology, 95(4), 311–327. https://doi.org/10.1139/cjpp-2016-0346
- McKinney, M. K., & Cravatt, B. F. (2003). Evidence for distinct roles in catalysis for residues of the serine-serine-lysine catalytic triad of fatty acid amide hydrolase. *Journal of Biological Chemistry*, 278(39), 37393–37399. https://doi.org/10.1074/jbc.M303922200
- Mor, M., Lodola, A., Rivara, S., Vacondio, F., Duranti, A., Tontini, A., ... Piomelli, D. (2008). Synthesis and quantitative structure-activity relationship of fatty acid amide hydrolase inhibitors: Modulation at the N-portion of biphenyl-3-yl alkylcarbamates. *Journal of Medicinal Chemistry*, 51(12), 3487–3498. https://doi.org/10.1021/jm701631z
- Mor, M., Rivara, S., Lodola, A., Plazzi, P. V., Tarzia, G., Duranti, A., ... Piomelli, D. (2004). Cyclohexylcarbamic acid 3'- or 4'-substituted biphenyl-3-yl esters as fatty acid amide hydrolase inhibitors: Synthesis, quantitative structure—activity relationships, and molecular modeling studies. *Journal of Medicinal Chemistry*, 47(21), 4998–5008. https://doi.org/10.1021/jm031140x
- Morena, M., Aukema, R. J., Leitl, K. D., Rashid, A. J., Vecchiarelli, H. A., Josselyn, S. A., & Hill, M. N. (2019). Upregulation of anandamide hydrolysis in the basolateral complex of amygdala reduces fear memory expression and indices of stress and anxiety. *Journal of Neuroscience*, 39(7), 1275–1292. https://doi.org/10.1523/jneurosci.2251-18.2018
- Mouro, F. M., Kofalvi, A., Andre, L. A., Baqi, Y., Muller, C. E., Ribeiro, J. A., & Sebastiao, A. M. (2019). Memory deficits induced by chronic cannabinoid exposure are prevented by adenosine A2AR receptor antagonism. *Neuropharmacology*, 155, 10–21. https://doi.org/10.1016/j.neuropharm.2019.05.003
- Mouro, F. M., Ribeiro, J. A., Sebastião, A. M., & Dawson, N. (2018). Chronic, intermittent treatment with a cannabinoid receptor agonist impairs recognition memory and brain network functional connectivity. *Journal of Neurochemistry*, 147(1), 71–83. https://doi. org/10.1111/jnc.14549
- Okamoto, Y., Wang, J., Morishita, J., & Ueda, N. (2007). Biosynthetic pathways of the endocannabinoid anandamide. *Chemistry and Biodiversity*, 4(8), 1842–1857. https://doi.org/10.1002/cbdv.20079 0155
- Pecic, S., Deng, S. X., Morisseau, C., Hammock, B. D., & Landry, D. W. (2012). Design, synthesis and evaluation of non-urea inhibitors of soluble epoxide hydrolase. *Bioorganic and Medicinal Chemistry Letters*, 22(1), 601–605. https://doi.org/10.1016/j.bmcl.2011.10.074
- Pecic, S., Makkar, P., Chaudhary, S., Reddy, B. V., Navarro, H. A., & Harding, W. W. (2010). Affinity of aporphines for the human 5-HT2A receptor: Insights from homology modeling and molecular docking studies. *Bioorganic and Medicinal Chemistry*, 18(15), 5562–5575. https://doi.org/10.1016/j.bmc.2010.06.043
- Pecic, S., McAnuff, M. A., & Harding, W. W. (2011). Nantenine as an acetylcholinesterase inhibitor: SAR, enzyme kinetics and molecular modeling investigations. *Journal of Enzyme Inhibition and Medicinal Chemistry*, 26(1), 46–55. https://doi.org/10.3109/14756 361003671078

- Pecic, S., Zeki, A. A., Xu, X., Jin, G. Y., Zhang, S., Kodani, S., ... Deng, S.-X. (2018). Novel piperidine-derived amide sEH inhibitors as mediators of lipid metabolism with improved stability. *Prostaglandins and Other Lipid Mediators*, 136, 90–95. https://doi.org/10.1016/j.prostaglandins.2018.02.004
- Pertwee, R. G. (2006). The pharmacology of cannabinoid receptors and their ligands: An overview. *International Journal of Obesity*, 30(Suppl 1), S13–S18. https://doi.org/10.1038/sj.ijo.0803272
- Pontius, J., Richelle, J., & Wodak, S. J. (1996). Deviations from standard atomic volumes as a quality measure for protein crystal structures. *Journal of Molecular Biology*, 264(1), 121–136. https://doi.org/10.1006/jmbi.1996.0628
- Reggio, P. H. (2010). Endocannabinoid binding to the cannabinoid receptors: What is known and what remains unknown. *Current Medicinal Chemistry*, 17(14), 1468–1486. https://doi.org/10.2174/09298 6710790980005
- Scherma, M., Masia, P., Satta, V., Fratta, W., Fadda, P., & Tanda, G. (2019). Brain activity of anandamide: A rewarding bliss? *Acta Pharmacologica Sinica*, 40(3), 309–323. https://doi.org/10.1038/s41401-018-0075-x
- Simon, V., & Cota, D. (2017). MECHANISMS IN ENDOCRINOLOGY: Endocannabinoids and metabolism: Past, present and future. European Journal of Endocrinology, 176(6), R309–R324. https://doi.org/10.1530/eje-16-1044
- Tarzia, G., Duranti, A., Tontini, A., Piersanti, G., Mor, M., Rivara, S., ... Piomelli, D. (2003). Design, synthesis, and structure-activity relationships of alkylcarbamic acid aryl esters, a new class of fatty acid amide hydrolase inhibitors. *Journal of Medicinal Chemistry*, 46(12), 2352–2360. https://doi.org/10.1021/jm021119g
- Thomas, B. F., & ElSohly, M. A. (2016). Biosynthesis and pharmacology of phytocannabinoids and related chemical constituents. In B. F.

- Thomas & M. A. ElSohly (Eds.), *The analytical chemistry of cannabis* (pp. 27–41). Amsterdam, the Netherlands: Elsevier.
- Ueda, N. (2002). Endocannabinoid hydrolases. Prostaglandins and Other Lipid Mediators, 68–69, 521–534. https://doi.org/10.1016/ S0090-6980(02)00053-9
- Vriend, G., & Sander, C. (1993). Quality control of protein models: Directional atomic contact analysis. *Journal of Applied Crystallography*, 26(1), 47–60. https://doi.org/10.1107/S002188989 2008240
- Wang, X., Sarris, K., Kage, K., Zhang, D. I., Brown, S. P., Kolasa, T., ... Stewart, A. O. (2009). Synthesis and evaluation of benzothiazole-based analogues as novel, potent, and selective fatty acid amide hydrolase inhibitors. *Journal of Medicinal Chemistry*, 52(1), 170–180. https://doi.org/10.1021/jm801042a

SUPPORTING INFORMATION

Additional supporting information may be found online in the Supporting Information section.

How to cite this article: Wilt SR, Rodriguez M, Le TNH, Baltodano EV, Salas A, Pecic S. Design, microwave-assisted synthesis, biological evaluation and molecular modeling studies of 4-phenylthiazoles as potent fatty acid amide hydrolase inhibitors. *Chem Biol Drug Des.* 2020;95:534–547. https://doi.org/10.1111/cbdd.13670